



HAL
open science

Aluminium competitive effect on rare earth elements binding to humic acid

Remi Marsac, Mélanie Davranche, Gérard Gruau, Aline Dia, Martine
Bouhnik-Le Coz

► **To cite this version:**

Remi Marsac, Mélanie Davranche, Gérard Gruau, Aline Dia, Martine Bouhnik-Le Coz. Aluminium competitive effect on rare earth elements binding to humic acid. *Geochimica et Cosmochimica Acta*, 2012, 89, pp.1-9. 10.1016/j.gca.2012.04.028 . hal-01904157

HAL Id: hal-01904157

<https://hal.science/hal-01904157>

Submitted on 24 Oct 2018

HAL is a multi-disciplinary open access archive for the deposit and dissemination of scientific research documents, whether they are published or not. The documents may come from teaching and research institutions in France or abroad, or from public or private research centers.

L'archive ouverte pluridisciplinaire **HAL**, est destinée au dépôt et à la diffusion de documents scientifiques de niveau recherche, publiés ou non, émanant des établissements d'enseignement et de recherche français ou étrangers, des laboratoires publics ou privés.

1 **Aluminium competitive effect on Rare Earth**
2 **Elements binding to humic acid**
3
4

5 Rémi Marsac, Mélanie Davranche*, Gérard Gruau,

6 Aline Dia and Martine Bouhnik-Le Coz
7
8
9

10
11 Géosciences Rennes, UMR 6118 CNRS - Université Rennes 1,

12 Campus de Beaulieu, 35042 Rennes Cedex, France
13
14
15

16 *Corresponding author: Tel +33 223 235 395; Fax: +33 223 236 090

17 E-mail address: melanie.davranche@univ-rennes1.fr
18

19 **Abstract-** Competitive mechanisms between rare earth elements (REE) and aluminium for
20 humic acid (HA) binding were investigated by combining laboratory experiments and
21 modeling to evaluate the effect of Al on REE-HA complexation. Results indicates that Al^{3+}
22 competes more efficiently with heavy REE (HREE) than with light REE (LREE) in acidic
23 (pH=3) and low REE/HA concentration ratio conditions providing evidence for the Al high
24 affinity for the few HA multidentate sites. Under higher pH - 5 to 6 - and high REE/HA
25 conditions, Al is more competitive for LREE suggesting that Al is bound to HA carboxylic
26 rather than phenolic sites. PHREEQC/Model VI Al-HA binding parameters were optimized to
27 simulate precisely both Al binding to HA and Al competitive effect on REE binding to HA.
28 REE-HA binding pattern could only be simulated reasonably well in the whole experimental
29 conditions studied only if ΔLK_{1A} was optimized (i.e. the parameter controlling width of the
30 distribution of log K around log K_{MA} , the median value). The present study provides
31 fundamental knowledge on Al binding mechanisms to HA. Aluminium competitive effect on
32 other cations binding to HA depends clearly on its affinity for carboxylic, phenolic or chelate
33 ligands, which is pH dependent. Under circumneutral pH conditions in natural waters, Al
34 should lead to LREE-depleted patterns since Al is not expected to bind efficiently neither to
35 HA phenolic groups nor to strong HA multidentate groups. As deduced from the behavior of
36 Al species, other potential competitor cations are expected to have their own competitive
37 effect on REE-HA binding. Therefore, in order to reliably understand and model REE-HA
38 pattern variations in natural waters, a precise knowledge of the exact behavior of the different
39 REE competitor cations is required. Finally, this study highlights the ability of the REE to be
40 used as a “speciation probe” to precisely describe cation interactions with HA as here
41 evidenced for Al.
42

43 Keywords: rare earth elements, aluminium, competition, complexation, humic acid,
44 PHREEQC, Model VI.

45 1. INTRODUCTION

46 Lanthanides represent a group of 14 naturally occurring elements, commonly denoted
47 as rare earth elements (REE), which bind strongly to natural dissolved organic matter (DOM)
48 (Takahashi et al., 1997; Viers et al., 1997; Dia et al., 2000; Tang and Johannesson, 2003;
49 Johannesson et al., 2004; Gruau et al., 2004; Davranche et al., 2005; Sonke and Salters, 2006;
50 Pourret et al., 2007a; Pédrot et al., 2008; Marsac et al., 2010; Yamamoto et al., 2010). The
51 unique property of REE is their chemically coherent behavior in natural systems. The regular
52 variations of their chemical behavior along the series can generate DOM/solution partition
53 coefficient (K_d) patterns with specific shapes depending on the binding conditions (i.e. the
54 nature of the functional group involved). REE binding to humic acid (HA) experiments
55 conducted under variable REE/HA ratios (defined as the REE to carbon molar ratio) and pH
56 conditions exhibit changes in K_d^{REE} pattern indication that REE can bind to different type of
57 HA sites (Marsac et al., 2011). More precisely, REE-HA binding experiments under acidic
58 and low REE/HA conditions yielded K_d^{REE} patterns showing an increase of heavy REE
59 (HREE) as compared to light REE (LREE). This feature is involved by the REE binding to
60 HA few strong sites that are similar to chelate ligands such as EDTA and have more affinity
61 for HREE than LREE (Sonke and Salters, 2006; Marsac et al., 2010; Yamamoto et al., 2010).
62 Experiments conducted at high REE/HA conditions showed K_d^{REE} pattern with an increase for
63 the middle REE (MREE) specific of REE binding with carboxylic ligands such as acetic acid
64 (Tang and Johannesson, 2003; Pourret et al., 2007b). This downward MREE concavity was
65 suggested to be developed through the REE binding with abundant and weak HA carboxylic
66 sites. This K_d^{REE} pattern dependence to REE/HA and involved HA binding site was

67 successfully modeled by Marsac et al. (2011) using the specific humic-ion binding model
68 (Model VI) developed by Tipping (1998). The modeling approach suggest that at high
69 REE/HA conditions, although LREE are dominantly (>80%) bound to carboxylic sites, a
70 majority of HREE (>80%) are bound to phenolic and carboxy-phenolic sites (Marsac et al.,
71 2011). The experimental and modeling results raise therefore the possibility that REE could
72 be used as a tool to determine which of the carboxylic, phenolic or chelate functional groups
73 are implicated in the binding of a given cation by HA. All cations able to compete with REE
74 for HA binding could not only involve a quantitative decrease of the complexed REE bound
75 to HA but also modify the REE-HA K_d pattern depending on their respective affinity for
76 carboxylic, phenolic or chelate HA sites. Conversely, variations of the REE-HA K_d pattern
77 patterns observed in presence of a competitive cation could provide additional clues to
78 explain why REE pattern variations occur in natural, organic-rich waters (Marsac et al., 2010,
79 and references therein).

80 In this respect, aluminium (Al) is of particular interest. Aluminium is abundant in
81 natural, organic-rich waters, specifically acidic water, with Al^{3+} activity up to around 10^{-3} mol
82 L^{-1} (Tipping, 2005). Moreover, Al has strong affinity for HA and is thus a strong competitor
83 for cations-HA binding including REE (Bidoglio et al., 1991; Tanizaki et al., 1992; Takahashi
84 et al., 1997; Dupré et al., 1999; Kinniburgh et al., 1999; Pinheiro et al., 2000; Tipping et al.,
85 2002; Lippold et al., 2005). The competitive binding of Al and the whole REE group has not
86 been experimentally studied. A common belief is that Al is preferentially bound to strong HA
87 sites and is therefore a stronger competitor for HREE than for LREE. As a consequence, Al
88 should induce a relative decrease of HREE in the K_d^{REE} pattern (Yamamoto et al., 2010; Tang
89 and Johannesson, 2010; Marsac et al., 2011). However, this stronger competition of Al for
90 HREE is opposite to Tipping et al. (2002) parameters of Model VI describing Al and REE

91 binding to HA. The ΔLK_2 parameter that defines the strength of HA multidentate sites are
92 $\Delta LK_2(\text{Al}) < \Delta LK_2(\text{LREE}) < \Delta LK_2(\text{HREE})$. Therefore, Model VI predicts a stronger
93 competitive effect of Al on LREE than on HREE.

94 In the present study, REE-Al-HA binding experiments were performed simultaneously
95 on the 14 naturally occurring REE over a range of metal loading and pH conditions. The aim
96 of this work is threefold: i) to experimentally investigate the competitive effects of Al on REE
97 complexation by HA in conditions that highlight the competition with the few strong
98 multidentate and phenolic groups, respectively; ii) to evaluate the ability of PHREEQC/Model
99 VI to predict the experimental data and to improve the quality of the modeling; iii) to test the
100 ability of the REE to be used as a fingerprint of the mechanisms of Al binding to HA.

101 **2. MATERIALS AND METHODS**

102 All chemicals used were of analytical grade, with all experimental solutions being
103 prepared with doubly-deionised water (Milli-Q system, Millipore™). Synthetic REE solutions
104 were prepared from a nitrate REE standard (10 mg L⁻¹, Accu Trace™ Reference Standard).
105 Polyethylene containers used to get REE-HA complexation equilibrium were all previously
106 soaked in 10% Ultrapure HNO₃ for 48h at 60°C, then rinsed with deionised water for 24h at
107 60°C. All experiments were performed at room temperature, i.e. 20°C ± 2.

108 **2.1. Humic acid**

109 Purified humic acid (HA) was obtained from synthetic Aldrich humic acid (Aldrich™,
110 H1, 675-2). The purification was performed with the protocol of Vermeer et al. (1998), except
111 that a tangential ultrafiltration step was added to remove any possible HA molecules <10 kDa
112 using a Labscale TFF system equipped with a Pellicon XL membrane (PLCGC10,
113 Millipore™). Humic acid was freeze-dried and stored in a glass container. Prior to use,

114 purified HA was solubilized overnight in a solution of 0.01 M NaCl at pH = 10 to ensure
115 complete dissolution (Vermeer et al., 1998). The pH was adjusted to 3 in the HA suspensions,
116 which were then filtered at 0.2 μ m to remove any potential precipitate and therefore to ensure
117 studying the same HA fraction in any experiments performed even at higher pH. The
118 dissolved organic carbon (DOC) concentration of the filtrates was then measured to assess the
119 true HA concentration of the experimental suspensions.

120 **2.2. Experimental set-up of the REE and Al binding to HA**

121 A standard batch equilibrium technique was used to study the competitive effect of Al
122 on REE binding by HA. The fourteen REE and Al were simultaneously added to HA
123 suspension set in a 10⁻² M (NaCl) electrolyte solution. Experimental suspensions were stirred
124 for 48 h to reach equilibrium according to the protocol defined by Pourret et al. (2007b). The
125 pH was monitored regularly with a combined Radiometer Red Rod electrode, calibrated with
126 WTW standard solutions (pH 4 and 7). The accuracy of pH measurements was ± 0.05 pH
127 units. At equilibrium (48 h), 10 mL of the suspension were sampled and ultra-filtered at 5 kDa
128 to separate the REE-HA and Al-HA complexes from the remaining inorganic REE and Al.
129 Ultrafiltrations were carried out by centrifuging the suspension aliquots through 15 mL
130 centrifugal tubes equipped with permeable membranes of 5 kDa pore size (Vivaspin 15RH12,
131 Sartorius). All the membranes used were first washed with 0.15 mol L⁻¹ HCl, then rinsed
132 twice with ultrapure water to minimize contamination. Centrifugations were performed using
133 a Jouan G4.12 centrifuge with swinging bucket rotor at 3000g for 30 min. The purification
134 step that consists in removing HA fractions <10 kDa ensures that no organic molecules pass
135 through the 5 kDa membrane at this stage of the experiments. All experiments were
136 performed in triplicate.

137 Two types of REE-Al competition experiments were performed. The first type was
138 performed at pH 3, under low REE/HA ($\Sigma[\text{REE}] = 1 \mu\text{M}$; $\text{DOC} = 9 \text{ mg L}^{-1}$; $\text{REE/HA} = 1.2$
139 $10^{-3} \text{ molREE/molC}$) and variable Al concentration (0 to $20 \mu\text{M}$) conditions. Under these
140 conditions, REE should be preferentially bound to HA by means of the few strong
141 multidentate sites occurring on them. The competition with Al for these sites, if occurring,
142 should result in a relative HREE depletion of $\log K_d^{\text{REE}}$ pattern (see above). This first series of
143 experiments was limited to pH 3 since higher pH values do not allow keeping measurable
144 amounts of REE in solution, due to the low REE/HA effect. The second series of experiments
145 was performed at variable pH ranging from 3 to 6, using higher REE/HA ($\Sigma[\text{REE}] = 10 \mu\text{M}$;
146 $\text{DOC} = 6.7 \text{ mg L}^{-1}$; $\text{REE/HA} = 2 \cdot 10^{-2} \text{ molREE/molC}$) and equal REE-Al concentrations
147 ($\Sigma[\text{REE}] = [\text{Al}] = 10 \mu\text{M}$). Reference experiments without Al were performed for
148 comparison. Due to higher REE/HA, REE are expected to be preferentially complexed by
149 carboxylic and phenolic functional groups in this second series of experiments, with an
150 expected increase of the phenolic/carboxylic ratio with increasing pH due to the higher proton
151 dissociation constant of phenolic groups (Marsac et al., 2011). Thus, this second series of
152 experiments was designed to provide information about the ability of Al to compete REE for
153 binding with HA phenolic sites. Speciation calculations carried out with PHREEQC showed
154 that all inorganic REE occur as free aqueous REE^{3+} species in the two series of experiments
155 (Tang and Johannesson, 2003; Pourret et al., 2007a; Marsac et al., 2010). The situation is
156 different for Al that can form hydroxide species and precipitate as $\text{Al}(\text{OH})_{3(\text{s})}$ in our
157 experimental condition. Stability constants between Al and hydroxides were taken from
158 minteq.v4 database. Aluminium activity was controlled by the precipitation of $\text{Al}(\text{OH})_3$,
159 following the reaction:



161 The REE complexation with HA is described using the apparent partition coefficient K_d , as
162 follows:

$$163 \quad K_d(\text{Ln}_i) = \frac{\mu\text{gLn}_i \text{ adsorbed L}^{-1}/\text{g DOC}}{\mu\text{gLn}_i^{3+} \text{ mL}^{-1}} \quad (2)$$

164 where $\text{Ln}_i = \text{La to Lu}$.

165 **2.3. Solution analysis**

166 Rare earth elements and Al concentrations were determined with an Agilent
167 Technologies™ HP4500 ICP-MS instrument. Ultrafiltrate, containing Al and REE inorganic
168 species, were injected directly after adding HNO_3 to a concentration of 0.37 N. The initial
169 suspensions were also analyzed to determine precisely total cation concentrations for each
170 experiment. The suspensions were first digested with sub-boiled nitric acid (HNO_3 14 N) at
171 100°C , and then resolubilized in HNO_3 0.37 N after complete evaporation, to avoid
172 interferences with organic carbon during mass analysis by ICP-MS. Quantitative analyses
173 were performed using a conventional external calibration procedure. Three external standard
174 solutions with REE and Al concentrations similar to the analyzed samples were prepared from
175 a multi-REE and an Al standard solution (Accu Trace™ Reference, 10 mg L^{-1} , USA). Indium
176 (In) was added to all samples as an internal standard at a concentration of $0.87 \mu\text{mol L}^{-1}$ (100
177 ppb) to correct for instrumental drift and possible matrix effects. Indium was also added to the
178 external standard solutions. Calibration curves were calculated from measured REE/In and
179 Al/In intensity ratios. As established from repeated analyses of multi-REE standard solution
180 (Accu Trace™ Reference, USA) and the SLRS-4 water standard, the instrumental error on
181 REE and Al analysis were below 3 and 5 %, respectively.

182 Dissolved organic carbon concentrations were determined using a Shimadzu 5000
183 TOC analyzer. The accuracy of DOC concentration measurements is estimated at $\pm 5\%$, as
184 determined by repeated analysis of freshly prepared standard solutions (potassium biphtalate).

185 **2.4. PHREEQC/Model VI**

186 Humic ion-Binding Model VI (hereafter referred to as Model VI) is a model
187 developed by Tipping (1998), which is implemented in the geochemical code WHAM 6. This
188 model was recently introduced into the PHREEQC (version 2) developed by Parkhurst and
189 Appelo (1999) for the entire REE series to improve REE-HA binding description, in
190 particular by removing the linear relationship between $\log K_{MA}$ and $\log K_{MB}$ (Marsac et al.,
191 2011). PHREEQC (version 2) is a computer code based on an ion-association aqueous model,
192 which was designed to perform speciation and saturation-index calculations in waters.

193 The humic-ion binding Model VI was developed by Tipping (1998). A thorough
194 description of Model VI can be found in Tipping (1998). The model is a discrete binding site
195 model which takes electrostatic interactions into account. Eight sites are considered and
196 divided into an equal number of type A sites (the weak acidic sites, commonly associated with
197 carboxylic functional groups) and type B sites (the strong acidic sites, commonly associated
198 with phenolic functional groups). There are n_A (mol g^{-1}) type A sites and $n_A/2$ type B sites.
199 Proton binding is described by the two median intrinsic constants (pK_A or pK_B) and two
200 parameters defining the spread of the equilibrium constants around the median (ΔpK_A or
201 ΔpK_B). The intrinsic equilibrium constants for metal ions (e.g. La^{3+} or Al^{3+}) and their first
202 hydrolysis product (e.g. LaOH^{2+} or AlOH^{2+}) binding are defined by two median constants
203 ($\log K_{MA}$ and $\log K_{MB}$), together with parameters that define the spread of the values around
204 the medians (ΔLK_{1A} and ΔLK_{1B}). By considering the results from many datasets, a universal
205 average value of ΔLK_1 was obtained for all cations (2.8), where $\Delta\text{LK}_1 = \Delta\text{pK}_A - \Delta\text{LK}_{1A} =$

206 $\Delta pK_B - \Delta LK_{1B}$ (appendix in Tipping et al., 2011). Some of the type A and type B
207 monodentate sites can form bi- and tridentate sites. The stability constants of these bi- and
208 tridentate sites are defined by the sum of the log K values of the monodentate sites of which
209 they are constituted. Cation-HA binding can occur through carboxylic groups (CG), carboxy-
210 phenolic groups (CPG) or phenolic groups (PG). A small part of the stability constants of
211 multidentate groups are increased by the ΔLK_2 parameter, the so-called "strong binding site
212 term" (Tipping, 1998). ΔLK_2 is attributed to the chelation effect or the participation of
213 ligands, such as the nitrogen-containing groups. Marsac et al. (2011) showed that to
214 accurately simulate REE-HA binding, ΔLK_2 parameter had to be optimized independently for
215 carboxylic (ΔLK_{2C}) and phenolic groups (ΔLK_{2P}). In the present paper, sites whose stability
216 constants with a cation depend on ΔLK_2 will be denoted as "strong multidentate sites". An
217 electrical double layer, where only counter-ions can accumulate, is also defined in the model.
218 The double layer thickness is set by the Debye-Hückel parameter $\kappa = (3.29 \times 10^9 \times I^{1/2})^{-1}$
219 (Appelo and Postma, 2005). The distribution of ions between the diffuse layer and the bulk
220 solution is calculated by a simple Donnan model. Intrinsic equilibrium constants are corrected
221 by the Boltzmann factor that depends on HA surface area which was determined to be equal
222 to 19000 m²/g at ionic strength of 0.01 (Marsac et al., 2011). In this study, HA was defined as
223 the SOLUTION_MASTER_SPECIES, SOLUTION_SPECIES and PHASES in the
224 PHREEQC database. The 80 types of site considered by Model VI to bind REE, Al and their
225 respective first hydrolysis products were defined as SURFACE_MASTER_SPECIES, and
226 their respective stability constants as SURFACE_SPECIES in the PHREEQC database. Al
227 hydroxide precipitation was also taken into account by defining Al(OH)₃(ha) - noted "ha" for
228 the experiments carried out in the presence of HA - in the PHASES block of PHREEQC
229 database. Aluminium activity was controlled by the precipitation of Al(OH)₃, following eq. 1.

230 With ultrafiltration at 5 kDa, Al-HA amount and precipitated as hydroxides cannot be
231 separately measured. The calculated amount of Al present in the fraction > 5kDa is defined
232 therefore by:

$$233 \quad \text{Al} > 5 \text{ kDa} = \text{Al(OH)}_{3(s)} + \text{Al-HA} \quad (4)$$

234 As a preliminary study, Al speciation in the fraction > 5kDa was simulated from pH = 3 to pH
235 = 6 in conditions comparable to our experiments (i.e. [DOC] = 6.7 mg L⁻¹; [Al] = 10 μM; IS =
236 0.01 M of NaCl). Simulation were performed using Model VI Al-HA binding parameters
237 determined by Tipping et al. (2002) and Log K_{SO} = 9 (eq. 1), which correspond to a 48h
238 equilibrated Al(OH)_{3(s)} (IUPAC, Stability Constants Database). Results are presented in
239 Figure 1 and show that Al³⁺ binding to HA is dominant at pH < 5. AlOH²⁺ binding to HA
240 ranges between 10% and 40% for pH > 4. Al(OH)_{3(s)} precipitates from pH = 5 and represents
241 60% of simulated Al in the fraction > 5kDa at pH = 6.

242 Errors between experiments and simulations were quantified by the root mean square
243 error of the regression (rmse), i.e. the sum of the squares of the differences between observed
244 and calculated log υ, where υ is the amount of REE bound to HA per gram of dissolved
245 organic carbon (DOC). To consider a fit as to be of good quality, two conditions had to be
246 fulfilled, namely: i) that the total rmse calculated from the whole experimental conditions and
247 REE were low, and ii) that the rmse values calculated for the fourteen REE were sufficiently
248 close to each other.

249 **3. RESULTS**

250 **3.1. Experimental Al competitive effect on REE-HA binding**

251 Figure 2 illustrates Al influence on log K_d^{REE} patterns at pH = 3 and low REE/HA (=
252 1.2 10⁻³). For [Al] = 0, REE-HA pattern increases regularly from La to Lu occurring through

253 preferential binding of REE to the low density strong multidentate sites with higher affinity
254 for HREE than for LREE (Yamamoto et al., 2010; Marsac et al., 2010). The presence of 1 μM
255 of Al strongly decreases the amount of REE bound to HA, while changing the $\log K_d^{\text{REE}}$
256 patterns which increases for MREE (MREE downward concavity). The Al concentration rise
257 from 1 to 20 μM decreases the amount of REE bound to HA, but does not influence the \log
258 K_d^{REE} pattern which remains essentially identical to that of the $[\text{Al}] = 1 \mu\text{M}$ experiment.
259 Therefore, Al appears to compete more efficiently with HREE than LREE in these
260 experiments, suggesting that Al has a higher affinity for strong multidentate sites. Because
261 less strong sites are available, REE bind mainly to weaker HA sites present in higher
262 concentration. At pH 3, the main REE-HA binding sites are thus carboxylic ligands whose
263 stability constants increase for MREE.

264 Figure 3a presents the percentage of REE bound to HA for $[\text{Al}] = 0$ and 10 μM for the
265 experiments conducted at high REE/HA ($2 \cdot 10^{-2}$) and variable pH (3 to 6). Without Al, around
266 30% of REE are bound to HA at pH = 3, a value that reaches 95% at pH = 6. The presence of
267 Al in equal amount than REE decreases the proportion of REE bound to HA. This decrease is
268 not uniform: Al competitive effect on REE-HA binding appears stronger between pH 4 and 5
269 than for lower pH. For pH > 5, $\text{Al}(\text{OH})_{3(\text{s})}$ precipitation might occur (fig. 1), decreasing
270 dissolved Al concentration and competition effect on REE-HA binding. Figure 3b compares
271 the $\log K_d^{\text{REE}}$ patterns at pH = 3, 4.5 and 6 for the REE-HA and REE-Al-HA experiments. As
272 previously observed at high REE/HA and whatever the pH can be, REE-HA experiments
273 result in $\log K_d^{\text{REE}}$ patterns with a MREE downward concavity, specific of the predominant
274 binding REE with weak, high density carboxylic HA sites (Tang and Johannesson 2003;
275 Pourret et al., 2007b; Marsac et al., 2010, and references therein). With Al, the LREE/HREE
276 balance is progressively modified with the increasing pH. At pH = 3, the competitive effect of

277 Al is more pronounced for the HREE than for the LREE, and at pH = 6, Al displaces more
278 strongly LREE than HREE (Fig. 3b). The corresponding change of the $\log K_d^{\text{REE}}$ pattern from
279 a $\log K_d^{\text{REE}}$ pattern presenting a MREE downward concavity at pH = 3 to a $\log K_d^{\text{REE}}$ pattern
280 slightly increasing for HREE at pH = 6 might be indicative of the type of HA sites bound to
281 Al and REE. At pH=3 with Al, the HREE depletion suggests the preferential binding of Al to
282 the few strong multidentate HA sites as for low REE/HA. Conversely, the LREE depletion or
283 HREE enrichment at pH = 6 might be due to the inability of Al to bind to HA phenolic sites.
284 Marsac et al. (2011) showed that about 80% of HREE are bound to HA phenolic and carboxy-
285 phenolic groups (i.e. phenol-containing groups) at pH=6. Conversely, at pH = 6, 80% LREE
286 are bound to HA carboxylic groups. Therefore, Al appears to be a strong competitor of REE
287 bound to COOH groups (i.e. mainly the LREE) than REE bound to phenol-containing groups
288 (i.e. mainly the HREE). In turn, $\text{Al}(\text{OH})_n^{(3-n)}$ species - which are the dominant Al species at
289 pH = 6 - present stronger affinity for carboxylic groups than for phenolic groups.

290 **3.2. Al and REE speciation modeling with PHREEQC/Model VI**

291 Our experiments at pH = 3, low REE concentrations and varying Al concentrations
292 show that Al^{3+} is a stronger competitor for HREE than LREE. In these conditions HREE are
293 mainly bound to strong multidentate sites whose stability constant with REE depends on
294 ΔKL_2 . This behaviour can not be simulated with Tipping et al. (2002) parameters for Al-HA
295 binding and Marsac et al. (2011) parameters for REE-HA binding in Model VI, as illustrated
296 on Figure 4a (dotted lines) for the experiment at low REE/HA, pH = 3 and $[\text{Al}] = 20 \mu\text{M}$.
297 Indeed here, $\Delta\text{KL}_2(\text{Al}^{3+})$ is very low (=0.46) and is, therefore, defined as a LREE competitor
298 rather than a HREE one. Consequently, Al-HA binding parameters in Model VI must be re-
299 evaluated. PHREEQC/Model VI requires the simultaneous adjustment of four parameters to

300 describe Al binding by HA, namely: $\log K_{MA}$ (for carboxylic groups), $\log K_{MB}$ (phenolic),
301 ΔLK_{2C} (strong multi-carboxylic) and ΔLK_{2P} (strong multi-phenolic) which can generate a
302 high degree of uncertainty on each parameter when individually taken. The Al-HA binding
303 parameters cannot be directly fitted from the Al-HA concentration since the possible presence
304 of $Al(OH)_{3(s)}$ in the >5 kDa fraction prevents the experimental quantification of Al-HA
305 concentration (Figure 1). However, the Al competitive effects on REE-HA binding pattern
306 and REE-HA concentrations provide important constraints on Al-HA binding parameters.

307 New Al-HA binding parameters in Model VI were determined by a data fitting
308 procedure, which consist in minimizing the RMSE. First, Al^{3+} parameters were determined
309 with our experiments at $pH = 3$, where other Al chemical species binding to HA and the
310 precipitation of $Al(OH)_{3(s)}$ can be neglected (Fig. 1). To define Al^{3+} as a stronger competitor
311 for HREE, $\log K_{MB}(Al^{3+})$ and $\Delta LK_{2P}(Al^{3+})$ (6.20 and 5.00, respectively) were determined
312 higher or close to the values for Lu (5.23 and 5.11, respectively) since Lu presents the highest
313 $\log K_{MB}$ and ΔLK_{2P} . The $\log K_{MA}(Al^{3+})$ was determined equal to 3 close to $\log K_{MA}(Lu)$
314 (3.16), which is the lowest $\log K_{MA}$ in the REE series. Because ΔLK_{2C} are similar for every
315 REE and range from 2.01 and 2.31 for La and Lu, respectively, $\Delta LK_{2C}(Al^{3+})$ was determined
316 equal to 1 to limit Al^{3+} competitive effect on LREE at low pH. Parameter values for Al-HA
317 binding are summarized in table 1. The newly optimized Al-HA binding parameters improve
318 the REE data fits at low REE/HA and $pH = 3$, compared with Tipping et al. (2002) parameter,
319 as illustrated for $[Al] = 20 \mu M$ on Figure 4a (dash-dotted line). Simulations at higher pH were
320 performed setting $\log K_{MA}$ and $\log K_{MB}$ for $AlOH^{2+}$ equal to Al^{3+} , according to Tipping et al.
321 (1998). However, to limit Al competition with HREE between pH 5 and 6, ΔLK_{2C} and ΔLK_{2P}
322 for $AlOH^{2+}$ were set equal to 0. $\log K_{SO}$ was also optimized and was found equal to 9.3,
323 which is closed to the literature data (i.e. $\log K_{SO} = 9$, IUPAC, Stability Constants Database).

324 RMSE for REE was equal to 0.07, which is low and should indicate a good fit. Figure 4b
325 presents experimental and simulated percentage of each REE bound to HA at pH = 6. It
326 shows that Al competitive effect on REE-HA binding is underestimated in these conditions
327 (dash-dotted line). Furthermore, the stronger competitive effect on LREE than on HREE can
328 not be reproduced. To improve the simulation of Al competitive effect on REE at pH > 4.5, a
329 higher value of log K_{MA} for $AlOH^{2+}$ than for Al^{3+} would be required (not shown), which is not
330 thermodynamically consistent.

331 As shown previously on REE-HA sorption edge (figure 3a), Al competitive effect on
332 REE-HA binding is low at pH < 4 and become stronger at pH > 4. From a modelling point of
333 view, this behaviour could be explained by different ΔLK_{1A} for Al and REE. Indeed, ΔLK_{1A}
334 represents the spread of stability constants between a cation and HA carboxylic groups around
335 log K_{MA} value. An increase of this spread decreases Al stability constants with half of HA
336 carboxylic groups, presenting the lower pK_a and log K with REE, and increases it for the
337 second half. Therefore, an increase of ΔLK_{1A} would lead to a decrease of Al-HA binding at
338 low pH and to an increase of Al-HA binding at high pH, accompanied with the corresponding
339 competitive effect on REE-HA binding. Model VI parameters for Al^{3+} determined above were
340 used as initial values for data fitting. Log K_{MA} and log K_{MB} for $AlOH^{2+}$ were set equal to Al^{3+}
341 ones but ΔLK_{2C} and ΔLK_{2P} were set equal to 0 for $AlOH^{2+}$. The best fit was obtained with
342 ΔLK_{1A} (Al) = 2.7, against -0.7 as determined by Tipping et al. (1998) for every cation (i.e.
343 $\Delta pK_a - \Delta LK_{1A} = 2.8$). The modification of ΔLK_{1A} implied some modification of other
344 parameters (log $K_{MA} = 3.3$, log $K_{MB} = 6.0$ and $\Delta LK_{2C} = 3$) as presented in table 1. The fit can
345 be considered of good quality because RMSE for REE is equal to 0.06. These parameters for
346 Al-HA binding allow simulating reasonably well REE-HA patterns at pH = 3 and low REE
347 concentration (Figure 4a, line) but also at pH = 6 and $[REE] = [Al]$ (Figure 4b, line). Figure 5

348 presents the fraction of Al > 5kDa versus the pH. The new parameters for Al can also
349 simulate reasonably well Al-HA binding.

350 **4. DISCUSSION**

351 The present study shows that Model VI Al-HA binding parameters have to be modifying
352 to be able to describe Al competitive effect on REE-HA binding. To test their reliability, the
353 new Model VI parameters for Al-HA binding determined in the present study were used to
354 simulate the experiments of (i) Kinniburgh et al. (1999), who studied Al-HA binding between
355 pH = 4 and 4.5 at various total Al concentration and (ii) Weng et al. (2002), who studied Al-
356 HA binding when HA is in contact with gibbsite between pH = 3.1 and 7. The conditions
357 studied by these authors provide a good test for the present Al parameters because they differ
358 strongly from our experiments. Figure 6 presents modeled versus experimental results of the
359 amount of Al bound to HA (in mol/kg). Our data at low REE/HA, pH = 3 and varying Al
360 concentrations are also presented. Data are close to the 1:1 line, showing a relatively good fit.
361 The total RMSE for Al in our experiments, Kinniburgh et al. (1999), and Weng et al. (2002)
362 is equal to 0.04. Therefore, the present Model VI Al-HA binding parameters derived from our
363 REE-Al competitive experiments allow simulating Al-HA binding in a wide range of pH and
364 Al to HA concentration ratio.

365 To date, Al competitive effect on cation-humics binding was generally studied at pH < 5
366 (Mota et al., 1996, Kinniburgh et al., 1999; Pinheiro et al., 2000). Model VI parameters for
367 Al-HA binding determined by Tipping et al. (2002) can reproduce reasonably well
368 experimental results. However, with these parameters at pH = 6, Al-HA binding is not strong
369 enough to limit Al(OH)_{3(s)} precipitation and Al competitive effect on other cations, such as
370 REE, is also limited (Fig. 4b). Furthermore, the present experimental results clearly show that

371 Al-HA interactions occur mainly by carboxylic HA sites rather than by phenolic HA sites.
372 Therefore, the chemical mechanisms defined by Tipping et al.'s (2002) set of Al-HA
373 parameters is not precise enough to simulate cation competition for HA binding under
374 environmental conditions. The new parameters determined in the present study describe more
375 precisely the mechanisms of Al binding to HA. Under the circumneutral pH conditions
376 characteristic of most natural waters, Al is therefore expected to be a significant competitor of
377 trace metals and radionuclides presenting a high binding affinity for HA carboxylic groups as
378 compared to phenolic groups such as LREE.

379 Numerous studies established that dissolved organic matter (DOM) controls the REE
380 speciation in natural, organic-rich waters (Bidoglio et al., 1991; Takahashi et al., 1997; Viers
381 et al., 1997; Dia et al., 2000; Johannesson et al., 2004; Gruau et al., 2004; Davranche et al.,
382 2005; Pourret et al., 2007a; Pédrot et al., 2008). Laboratory experiments here performed as
383 well as previous studies meanwhile established that HA binding has the potential of
384 fractionating REE depending on the involved HA binding sites and REE/HA ratio (Sonke and
385 Salters, 2006, Pourret et al., 2007b; Yamamoto et al., 2010; Marsac et al., 2010; 2011). For
386 low REE/HA, when REE-HA binding occurs mainly through strong multidentate sites, REE
387 patterns of natural, organic-rich waters are expected to show a progressive increase from La to
388 Lu. By contrast, when REE-HA binding is dominated by weak carboxylic sites (i.e. for high
389 REE/HA), patterns are expected to exhibit a MREE downward concavity (Yamamoto et al.,
390 2010; Marsac et al. 2010). By compiling data from natural, organic-rich waters, Marsac et al.
391 (2010) recently showed that REE patterns effectively displayed variations that could be partly
392 due to the REE/HA (or metal loading) effect. The true occurrence of this effect is however
393 challenged by other mechanisms able to potentially fractionate REE. The competitive effect
394 generated by other cations such as Al and Fe is one of possible mechanisms (Tang and

395 Johannesson, 2010). Yamamoto et al. (2010) suggested that even low concentrations of Al
396 and Fe could delete the above “low REE/HA” fractionation process. The experiments at pH 3
397 and low REE/HA reported in the present study show that Al competition has effectively the
398 potential of limiting the higher HREE-HA binding confirming this suggestion. However, at
399 pH > 5, the contrary is observed. Aluminium occurrence decreases LREE binding to HA.
400 Therefore, these results show that the Al binding to HA in circumneutral waters could
401 promote HREE enrichment in the dissolved fraction (i.e. < 0.2 μM) due to HREE higher
402 affinity for HA binding as compared to that of LREE. In other words, Al competition with
403 REE at circumneutral pH enhances the metal loading effect on REE-HA pattern.

404 The present study confirms that the REE-HA pattern depends on the REE speciation on
405 HA and can be used as a fingerprint of the dominant HA binding sites in given pH or
406 REE/HA conditions. Modification of REE speciation on HA - and thus in REE-HA pattern -
407 is expected to occur not only in response to variations of REE/HA ratio but, to the occupation
408 of HA sites by competitor cations, such as Al. Marsac et al. (2011) suggested that different
409 effects on REE-HA pattern are anticipated depending on the affinity of competitor cations for
410 carboxylic and phenolic sites. At pH > 5, the competitive effect of Al, occurring mainly for
411 LREE, confirms this hypothesis. Up to now, predictions of REE speciation in natural,
412 organic-rich waters were performed using Model VI (or the previous version Model V), using
413 generic parameters for other cations (Tang and Johannesson, 2003; Pourret et al., 2007b).
414 These predictions could only give information about the total amount of REE displaced by the
415 competitor cation but, not on the competition effect on the 14 REE taken individually.
416 Generic cation-HA binding parameters commonly used in Model VI are those determined
417 initially by Tipping (1998) applying a linear relationship between carboxylic and phenolic
418 parameters. The cations present therefore the same relative affinity for HA carboxylic and

419 phenolic functional groups. Even if this assumption gives satisfactory modeling results for
420 competitive experiments between two cations (Tipping, 1998; Peters et al., 2001; Tipping et
421 al., 2002), the present REE-Al competition study shows that these generic parameters are not
422 mechanistically sufficient to describe the effects of cation competition on REE pattern. To use
423 geochemical models as a reliable tool to describe REE patterns in natural, organic rich-waters,
424 a more accurate description of the different competitor cations binding behavior with HA is
425 clearly required. In this perspective, further experimental studies of cation-REE competitive
426 binding to HA are required, which might in turn take benefit of the “REE fingerprint” set up
427 in this and previous studies to further highlight the complex mechanisms involved in cation
428 binding to HA.

429 5. CONCLUSION

430 The competition experiments between REE and Al show different Al competition
431 effects depending on the pH and the REE/HA ratio. Under acidic (pH = 3) and low REE/HA
432 conditions, Al^{3+} as the dominant Al species compete more strongly with HREE than with
433 LREE. Therefore, Al^{3+} has high affinity for the few amount of HA strong multidentate sites.
434 Under higher pH ranging from 5 to 6 and higher REE/HA conditions, the competition is more
435 pregnant with meaning for LREE than for HREE, suggesting a strong interaction of Al with
436 HA carboxylic groups. PHREEQC/Model VI Al-HA binding parameters were optimized to
437 simulate precisely both Al binding to HA and its competitive effect on REE. REE-HA
438 binding pattern could only be simulated reasonably well in the whole experimental conditions
439 studied only if ΔLK_{1A} was optimized (i.e. the parameter controlling width of the distribution
440 of log K around log K_{MA} , the median value). The present study provides fundamental
441 knowledge on Al binding mechanisms to HA. Aluminium competitive effect on other cations
442 binding to HA depends clearly on its affinity for carboxylic, phenolic or chelate ligands,

443 which is pH dependent. From our experimental results, we can conclude that, the presence of
444 Al should enhance the metal loading effect on REE-HA pattern (i.e. an increase from LREE
445 to HREE) since Al is not expected to bind efficiently neither to HA phenolic groups nor to the
446 low amount of HA strong multidentate groups. As deduced from the different behavior
447 depicted by the different Al species, other potential competitor cations are expected to have
448 their own competitive effect on REE-HA binding. Therefore, a precise knowledge of the exact
449 behavior of the different REE competitor cations is required in order to reliably understand
450 and model REE-HA pattern variations in natural waters. Finally, the REE-HA patterns
451 resulting from Al competition were used as a probe to evaluate Al ability to bind to different
452 HA sites (carboxylic, phenolic or chelate ligands). This ability of the REE to be used as a
453 "speciation probe" could be applied to other cations in order to precisely describe their
454 interactions with HA.

455

456 **Acknowledgments.** We thank Pr. Johnson Haas (AE), Dr. Jianwu Tang and two anonymous
457 reviewers for their important comments. This research was funded by the French ANR,
458 through the "Programme Jeunes Chercheuses - Jeunes Chercheurs: SURFREE (Rare earth
459 elements partitioning at solid-water interface: Impact on REE geochemical behaviour and
460 tracing properties)".

461

REFERENCES

- 462
- 463 Appelo C. and Postma D. (2005) *Geochemistry, groundwater and pollution* (2nd edition).
464 Taylor & Francis, p. 595.
- 465 Bidoglio G., Grenthe I., Qi P., Robouch P. and Omentto N. (1991) Complexation of Eu and
466 Tb with fulvic acids as studied by time-resolved laser-induced fluorescence. *Talanta* **38**
467 (9), 999–1008.
- 468 Davranche M., Pourret O., Gruau G., Dia A. and Le Coz-Bouhnik M. (2005) Adsorption of
469 REE(III)–humate complexes onto MnO₂: experimental evidence for cerium anomaly and
470 lanthanide tetrad effect suppression. *Geochim. Cosmochim. Acta* **69**, 4825–4835.
- 471 Dia A., Gruau G., Olivie-Lauquet G., Riou C., Molénat J. and Curmi P. (2000) The
472 distribution of rare-earths in groundwater: assessing the role of source-rock composition,
473 redox changes and colloidal particles. *Geochim. Cosmochim. Acta* **64**, 4131–4151.
- 474 Dupré L., Viers J., Dandurand J.-L., Polvé M., Bénézech P., Vervier P. and Braun J.-J. (1999)
475 Major and trace elements associated with colloids in organic-rich river waters:
476 Ultrafiltration of natural and spiked solutions. *Chem. Geol.* **160**, 63–80.
- 477 Elderfield H., Upstill-Goddard R. and Sholkovitz E.R. (1990) The rare earth elements in
478 rivers, estuaries, and coastal seas and their significance to the composition of ocean
479 waters. *Geochim. Cosmochim. Acta* **54**, 971–991.
- 480 Gruau G., Dia A., Olivie-Lauquet G., Davranche M. and Pinay G. (2004) Controls on the
481 distribution of rare earth elements in shallow groundwaters. *Wat. Res.* **38**, 3576-3586.
- 482 IUPAC (2001) *IUPAC Stability Constants Database*. Version 5.4, IUPAC and Academic 584
483 Software (acadsoft@bcs.org.uk).

484 Johannesson K.H., Tang J., Daniels J.M., Bounds W.J. and Burdige D.J. (2004) Rare earth
485 element concentrations and speciation in organic rich blackwaters of the Great Dismal
486 Swamp, Virginia, USA. *Chem. Geol.* **209**, 271–294.

487 Kinniburgh D. G., van Riemsdijk W. H., Koopal L. K., Borkovec M., Benedetti M. F. and
488 Avena M. J. (1999) Ion binding to natural organic matter: competition, heterogeneity,
489 stoichiometry and thermodynamic consistency. *Colloid Surf. A* **151**, 147–166.

490 Lippold H., Mansel A. and Kupsch H. (2005) Influence of trivalent electrolytes on the humic
491 colloid-borne transport of contaminant metals: competition and flocculation effects.
492 *Journal of Contaminant Hydrology* **76**, 337– 352.

493 Marsac R., Davranche M., Gruau G. and Dia A. (2010) Metal loading effect on rare earth
494 element binding to humic acid: Experimental and modeling evidence. *Geochim.*
495 *Cosmochim. Acta* **74**, 1749-1761.

496 Marsac R., Davranche M., Gruau G, Bouhnik-Le Coz M. and Dia A. (2011) An improved
497 description of the interactions between rare earth elements and humic acids by modeling.
498 *Geochim. Cosmochim. Acta* (in press).

499 Mota A.M., Rato A., Brazia C. and Simoes Gonçalves M.L. (1996) Competition of Al³⁺ in
500 complexation of humic matter with Pb²⁺: a comparative study with other ions. *Environ.*
501 *Sci. Technol.* **30**, 1970-1974.

502 Parkhurst D.L. and Appelo C.A.J. (1999) User's guide to PHREEQC (Version 2) - a computer
503 program for speciation, batch reaction, one-dimensional transport and inverse
504 geochemical calculation. Water-resources Investigation Report 99-4259, USGS, Denver,
505 Colorado, p. 312.

506 Pédrot M., Dia A., Davranche M., Bouhnik-Le Coz M., Henin O. and Gruau G. (2008)
507 Insights into colloid-mediated trace element release at soil/water interface. *J. Coll. Int.*
508 *Sci.* **325**, 187-197.

509 Peters A., Hamilton-Taylor J. and Tipping E. (2001) Americium binding to humic acid.
510 *Environ. Sci. Technol.* **35**, 3495–3500.

511 Pinheiro J.P., Mota A.M. and Benedetti M.F. (2000) Effect of aluminum competition on lead
512 and cadmium binding to humic acids at variable ionic strength. *Environ. Sci. Technol.* **34**,
513 5137-5143.

514 Pourret O., Davranche M., Gruau G. and Dia A. (2007a) Organic complexation of rare earth
515 elements in natural waters: evaluating model calculations from ultrafiltration data.
516 *Geochim. Cosmochim. Acta* **71**, 2718–2735.

517 Pourret O., Davranche M., Gruau G. and Dia A. (2007b) Rare earth complexation by humic
518 acid. *Chem. Geol.* **243**, 128-141.

519 Sonke J.E. and Salters V.J.M. (2006) Lanthanide–humic substances complexation. I.
520 Experimental evidence for a lanthanide contraction effect. *Geochim. Cosmochim. Acta*
521 **70**, 1495–1506.

522 Takahashi Y., Minai Y., Ambe S., Makide Y., Ambe F. and Tominaga T. (1997)
523 Simultaneous determination of stability constants of humate complexes with various
524 metal ions using multitracer technique. *The Science of the Total Environment* **198**, 61–71.

525 Tang J. and Johannesson K.H. (2003) Speciation of rare earth elements in natural terrestrial
526 waters: assessing the role of dissolved organic matter from the modeling approach.
527 *Geochim. Cosmochim. Acta* **67**, 2321–2339.

528 Tang J. and Johannesson K.H. (2010) Ligand extraction of rare earth elements from aquifer
529 sediments: Implications for rare earth element complexation with organic matter in
530 natural waters. *Geochim. Cosmochim. Acta* **74**, 6690-6705.

531 Tanizaki Y., Shimokawa T. and Nakamura M. (1992) Physicochemical speciation of trace
532 elements in river waters by size fractionation. *Environ. Sci. Technol.* **26**, 1433–1444.

533 Tipping E. (1998) Humic ion-binding model VI: an improved description of the interactions
534 of protons and metal ions with humic substances. *Aquatic Geochemistry* **4**, 3–48.

535 Tipping E. (2005) Modeling Al competition for heavy metal binding by dissolved organic
536 matter in soil and surface waters of acid and neutral pH. *Geoderma* **127**, 293–304.

537 Tipping E., Rey-Castro C., Bryan S. E., and Hamilton-Taylor J. (2002) Al(III) and Fe(III)
538 binding by humic substances in freshwaters and implications for trace metal speciation.
539 *Geochim. Cosmochim. Acta* **66**, 3211–3224.

540 Tipping E., Lofts S. and Sonke J.E. (2011) Humic Ion-Binding Model VII: a revised
541 parameterisation of cation-binding by humic substances. *Environ. Chem.* **8**, 225–235.

542 Vermeer A.W.P., Van Riemsdijk W.H. and Koopal L.K. (1998) Adsorption of humic acid to
543 mineral particles. 1. Specific and electrostatic interactions. *Langmuir* **14**, 2810–2819.

544 Viers J., Dupré B., Polvé M., Schott J., Dandurand J.-L. and Braun J.J. (1997) Chemical
545 weathering in the drainage basin of a tropical watershed (Nsimi–Zoetele site, Cameroon):
546 comparison between organic poor and organic-rich waters. *Chem. Geol.* **140**, 181–206.

547 Weng L., Temminghoff E.J.M. and Van Riemsdijk W.H. (2002) Aluminum speciation in
548 natural waters: measurement using Donnan membrane technique and modeling using
549 NICA-Donnan. *Water Research* **36**. 4215-4226.

550 Yamamoto Y., Takahashi Y. and Shimizu H. (2010) Systematic change in relative stabilities
551 of REE-humic complexes at various metal loading levels. *Geochemical Journal* **44**, 39-63.

552

553 **Table and Figure Captions**

554

555 **Table 1.** $\log K_{MA}$, $\log K_{MB}$, ΔLK_{2C} and ΔLK_{2P} for Al^{3+} and $AlOH^{2+}$ determined by
556 Tipping et al. (2002) and fitted from the present experimental data using PHREEQC/Model
557 VI adjusting or not the parameter ΔLK_{1A} . (*) In the present study ΔLK_{2C} and ΔLK_{2P} for
558 $AlOH^{2+}$ were set equal to 0.

559

560 **Figure 1.** Preliminary modeling study of Al speciation in the fraction $> 5kDa$ (i.e. Al-
561 HA + $Al(OH)_{3(s)}$) calculated with PHREEQC/Model VI for $[DOC] = 6.7 \text{ mg L}^{-1}$, $[Al] = 10$
562 μM , IS = 0.01 M (NaCl) and pH ranging from 3 to 6. Model VI Al-HA binding parameters
563 were determined by Tipping et al. (2002).

564

565 **Figure 2.** $\log K_d^{REE}$ patterns for REE, Al competitive binding to HA experiments at
566 pH 3 and low REE/HA ratios ($1.2 \cdot 10^{-3} \text{ molREE/molC}$) for $[Al] = 1$ and $20 \mu M$. Error bars
567 represent standard deviation from triplicates (can be hidden by symbols).

568

569 **Figure 3.** REE-HA binding for high REE/HA experiments: (a) effect of Al
570 concentration on the % of REE bound to HA relative to pH. (b) $\log K_d^{REE}$ patterns with and
571 without Al relative to pH.

572

573 **Figure 4.** REE percentage bound to HA from experimental data and simulation using
574 PHREEQC/Model VI, either in using Tipping et al. (2002) parameters for Al-HA binding
575 (dotted line), optimized parameters without optimizing ΔLK_{1A} (dash-dotted line) or
576 optimizing ΔLK_{1A} (line). (a) refers to the experiment conducted at pH 3, low REE/HA and

577 [Al] = 20 μM , whereas (b) refers to the experiment performed at pH = 6, high REE/HA and
578 with $\Sigma[\text{REE}] = [\text{Al}] = 10 \mu\text{M}$.

579

580 **Figure 5.** Comparison between experimental and simulated percentage of Al present
581 in the > 5 kDa fraction for experiments at $\Sigma[\text{REE}] = [\text{Al}] = 10\mu\text{M}$, $[\text{DOC}] = 6.7 \text{ mg L}^{-1}$ and
582 pH 3-6.

583

584 **Figure 6.** Comparison between experimental and simulated amount of Al bound to
585 HA, using optimized PHREEQC/Model VI Al-HA parameters, for literature data and the
586 present study data at pH 3 and low REE/HA.

587

588

589

Parameters for Al^{3+} and AlOH^{2+}	Tipping et al. (2002) $\Delta\text{LK}_{1A} = -0.7$	Present study $\Delta\text{LK}_{1A} = -0.7$	Present study $\Delta\text{LK}_{1A} = 2.7$ (adopted)
$\text{Log } K_{MA}$	2.60	3.00	3.30
$\text{Log } K_{MB}$	7.66	6.20	6.00
$\Delta\text{LK}_{2C}^{(*)}$	0.46	1.00	3.00
$\Delta\text{LK}_{2P}^{(*)}$	0.46	6.00	6.00

590

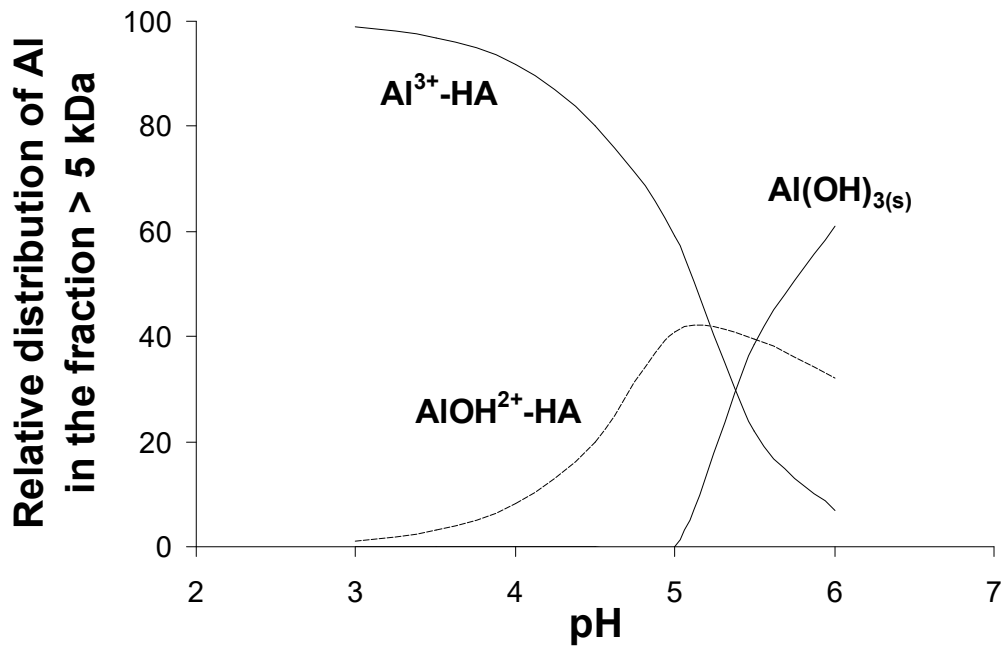
591

592

Table 1

593

594



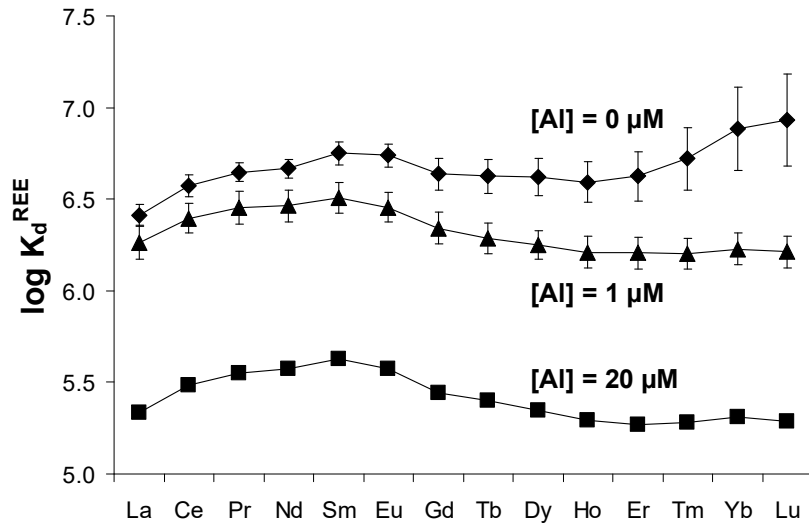
595

596

597

598

Figure 1

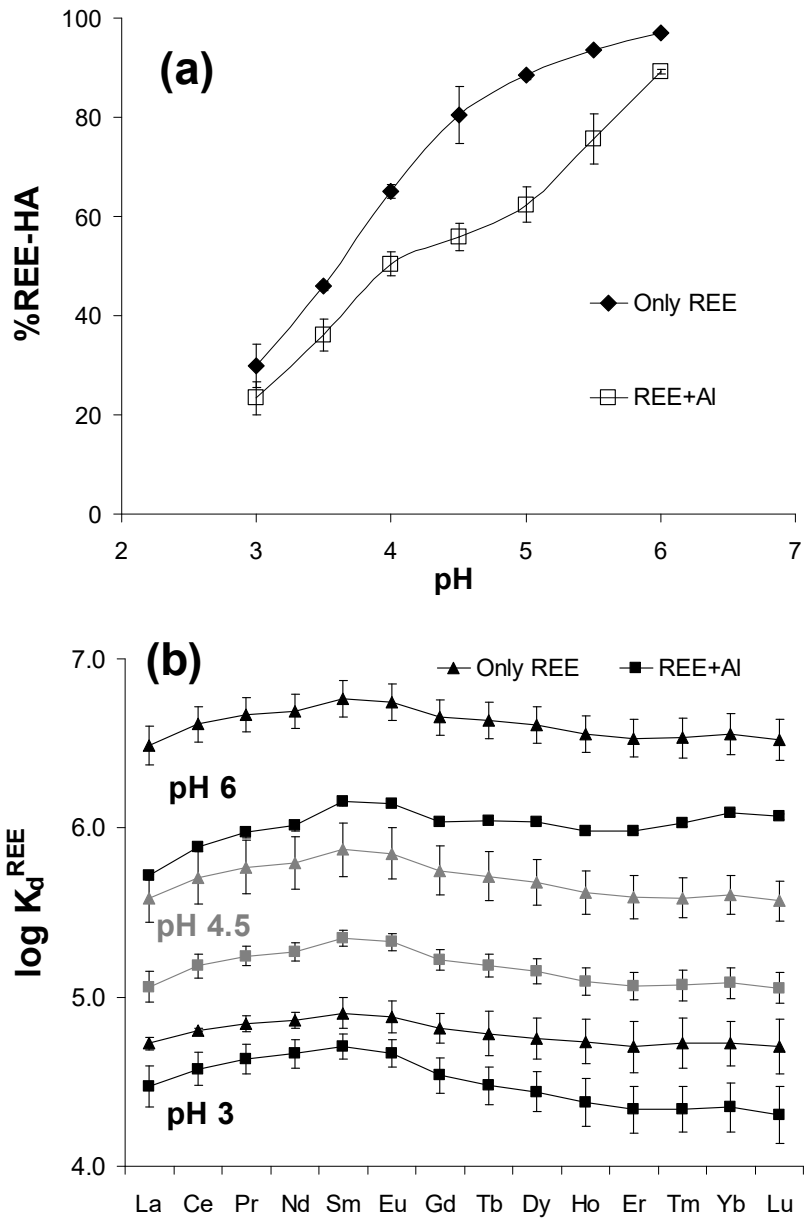


599

600

601

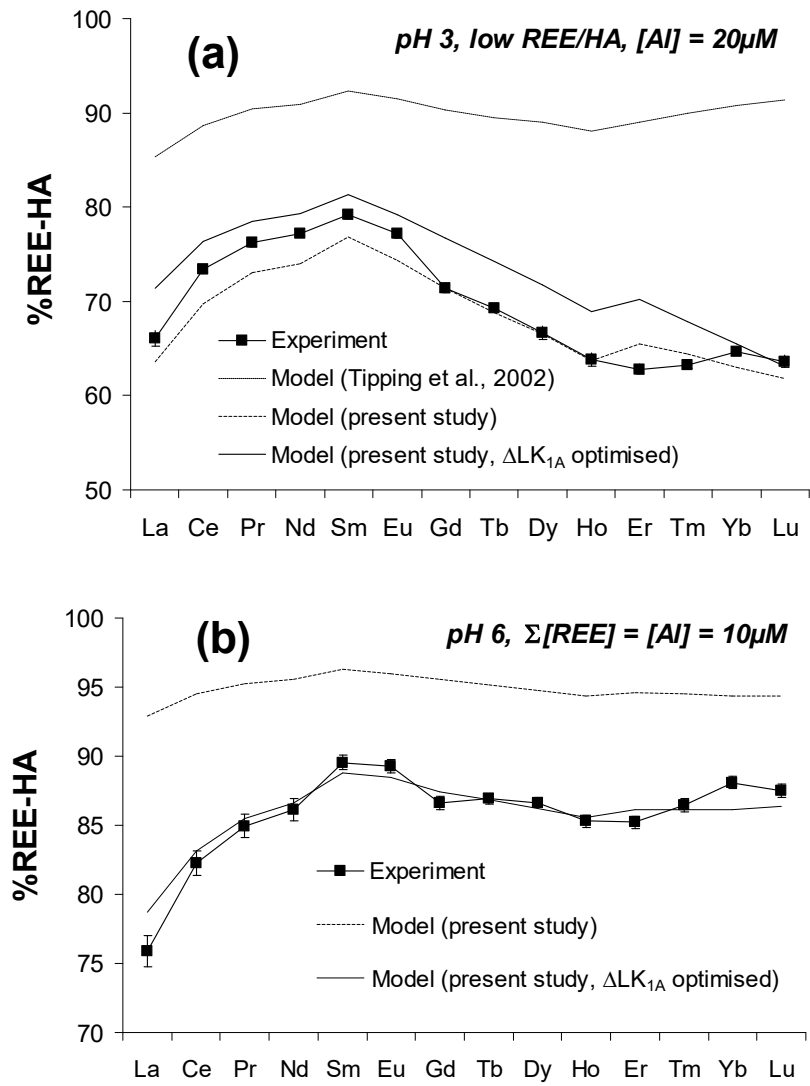
Figure 2



602

603

Figure 3



604

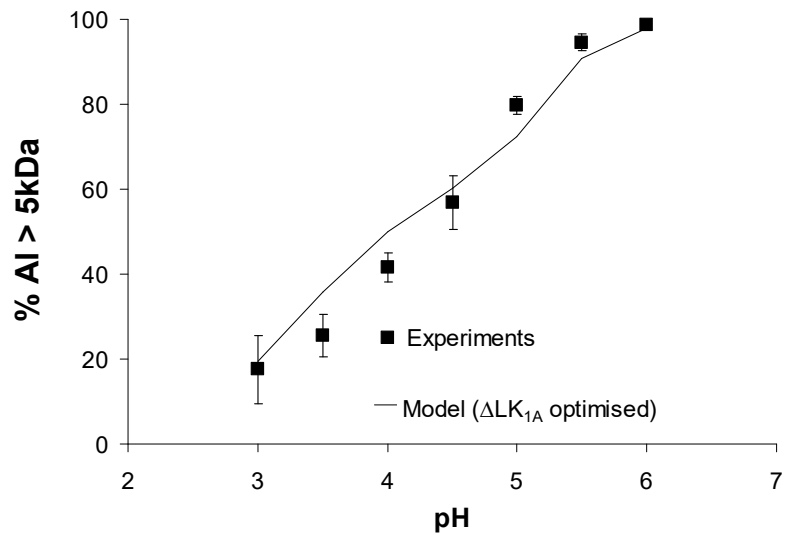
605

606

607

Figure 4

608



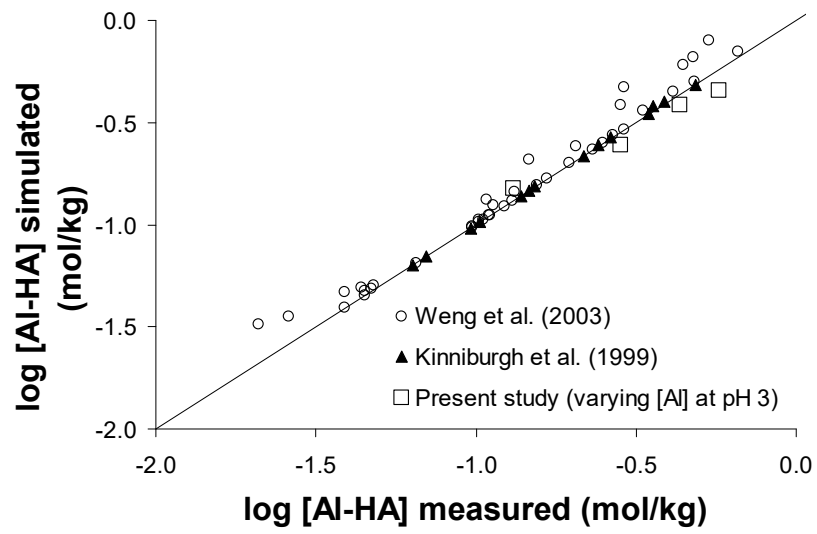
609

610

Figure 5

611

612



613

614

Figure 6